XLVI CILAMCE
VITÓRIA - ES - BRAZIL - 2025
XLVI IBERO-LATIN AMERICAN CONGRESS ON COMPUTATIONAL METHODS IN ENGENEERING

A Technique for Synthesizing Spectrum-Compatible Artificial Ground Motions

Daniel B. M. Matos[1], Juan F. V. Ospina[1], Letícia F. F. Miguel[2]

[1]*Postgraduate Program in Civil Engineering (PPGEC), Federal University of Rio Grande do Sul (UFRGS)*
Av. Osvaldo Aranha, 99, 90035-190, Porto Alegre-Rio Grande do Sul, Brazil
daniel.matos@ufrgs.br, juan.vallejo@ufrgs.br
[2]*Department of Mechanical Engineering (DEMEC), Postgraduate Program in Mechanical Engineering (PROMEC), Postgraduate Program in Civil Engineering (PPGEC) Federal University of Rio Grande do Sul (UFRGS)*
Av. Sarmento Leite, 425, 90050-170, Porto Alegre-Rio Grande do Sul, Brazil
letffm@ufrgs.br

Abstract. Contemporary seismic engineering relies heavily on nonlinear dynamic analyses to accurately assess the structural safety of essential infrastructure such as hospitals, bridges, and emergency operation centers, where estimating collapse probability and verifying serviceability levels are critical. However, pseudo-acceleration response spectra prescribed by standards like Eurocode 8, NSR-10, and NBR 15421 lack temporal information, limiting the ability to represent the evolution of seismic loads and to capture key phenomena such as stiffness degradation, damage accumulation, and stress redistribution. In this context, the generation of artificial seismic records emerges as a viable alternative for time-domain analyses. Although classical approaches such as the Kanai-Tajimi stochastic modelKanai [1], Tajimi [2] are widely adopted for their simplicity, they show poor spectral fidelity to target design spectra. This study proposes the Clough and Penzien methodologyClough and Penzien [3], a linear stochastic approach based on dual filtering, as a precise and conceptually robust solution. Preliminary results show that the synthetic accelerograms generated with this method exhibit strong spectral alignment with normative spectra, meeting both spectral and temporal requirements. Therefore, the proposed methodology is suitable for advanced seismic design and nonlinear structural response assessments.

Keywords: Artificial seismic records, Pseudo-acceleration spectra, Time-domain analysis)

1 Introduction

Modern seismic engineering increasingly relies on nonlinear dynamic analysis to accurately simulate the time-dependent structural response under realistic earthquake demands. While static pushover methods are still used for preliminary evaluations, they fall short in capturing higher-mode effects and progressive failure mechanisms (Krawinkler and Seneviratna [4]). Because nonlinear behavior invalidates the superposition principle, such analyses must be performed in the time domain(Chopra [5]). Within this context, real and synthetic accelerograms are essential tools for performance-based assessment, enabling the modeling of key post-elastic phenomena such as stiffness degradation, damage accumulation, and hysteretic energy dissipation (e.g., Schneider et al. [6], Wang et al. [7], Long et al. [8], Zhang et al. [9], Chy et al. [10]).

A common strategy in seismic assessment is the use of real ground motion records, especially from local accelerographic networks, as they reflect site-specific soil conditions and energy content. For instance, Miguel et al. [11] scaled records from Cúcuta, Colombia, to assess building reliability under increasing PGA levels. While such signals enhance realism and response fidelity, their long durations and high sampling rates can impose significant computational costs. Additionally, in regions with low seismicity or limited instrumentation, the lack of representative records introduces uncertainty and limits their applicability.

Dress the limitations of real records, artificial ground motion generation has become an essential complementary strategy in seismic analysis. Early models simulated earthquake excitation as stationary white noise (Housner [12], Bycroft [13]), later refined by the Kanai–Tajimi model (Kanai [1], Tajimi [2]), which filters white noise through a single-degree-of-freedom (SDOF) system to reproduce site-specific soil resonance effects—a formulation that became a cornerstone in stochastic modeling. Subsequent developments introduced nonstationarity through envelope functions (Shinozuka and Jan [14]), wavelet transforms (Conte and Peng [15]), and empirical

mode decomposition, as in Yamamoto and Baker [16], improving the representation of the time-varying spectral content of real ground motions. Despite these advances, challenges persist: many methods struggle to match the pseudo-acceleration spectra required by modern seismic codes (Chiesa and Fadel Miguel [17]), and attempts to control signal duration often compromise the statistical and dynamic consistency of the synthetic accelerograms as can be seen in Yamamoto and Baker [16].

To address these limitations, this study presents a synthetic ground motion generation method based on the framework of Clough and Penzien [3], capable of producing artificial accelerograms with high spectral fidelity to both recorded motions and design spectra. A key advantage lies in its ability to generate shorter-duration signals that retain the nonstationary and stochastic characteristics essential for nonlinear time-history analysis, thus reducing computational cost without compromising accuracy. Initial results show strong agreement between synthesized and target spectra, making the method a practical and efficient alternative—particularly useful in performance-based assessments and scenarios with limited access to real seismic records.

2 Accelerogram Generation Method Based on Clough and Penzien

This section implements the artificial accelerogram generation methodology described in Chapter 25 *Dynamics of Structures* by Clough and Penzien [3], focusing on the generation of artificial seismic accelerograms using stochastic processes.

The process begins by generating N random numbers uniformly distributed in the interval $[0, 1]$ For computational efficiency, N is typically chosen as a power of 2. These values form the vector:

$$\vec{n} = [n_1, n_2, n_3, ..., n_N] \tag{1}$$

Once the values of x are determined, radim number pairs are generated using eq. (2) and eq. (3). In this way, the resulting values of y follow a Gaussian distribution with zero mean and unit standard deviation:

$$y_i = \sqrt{-2 \ln x_i} \cos 2\pi x_{i+1} \tag{2}$$

$$y_{i+1} = \sqrt{-2 \ln x_i} \sin 2\pi x_{i+1} \tag{3}$$

To express y as a time-dependent function $y(t)$ time vector t is defined such that its elements are equally spaced by a time increment dt The initial value of y at $t = 0$ is set to zero, i.e., $y_0 = 0$.To better represent a seismic signal, the function $y(t)$ must be converted into a nonstationary signal$z(t)$ using an envelope function $f(t)$, as shown in eq. (4):

$$z(t) = y(t)f(t). \tag{4}$$

Here, $f(t)$ modulates the amplitude of the signal over time, simulating the energy release pattern of real earthquakes. Several envelope functions have been proposed in the literature (e.g.,Jennings et al. [18]). In this study, the envelope function defined by Ruiz and Penzien [19] is adopted due to its effectiveness and widespread use in seismic simulations.

$$f(t) = a_1 t e^{-a_2 t} \tag{5}$$

where the constants a_1 and a_2 are defined according to the desired seismic characteristics, such as magnitude and epicentral distance .

To adjust the frequency content of the signal $z(t)$, two filters are applied: the first, based on the Kanai–Tajimi model, amplifies frequencies near a target frequency ω_1; the second attenuates the low-frequency components near ω_2. For this purpose, it is necessary to define $Z(i\omega)$ as the Fourier transform of the nonstationary signal $z(t)$. The filtering process is then expressed as:

$$B(i\omega) \equiv Z(i\omega)H_1(i\omega)H_2(i\omega), \tag{6}$$

$$H_1(i\omega) = \frac{1 + 2i\xi_1 \frac{\omega}{\omega_1}}{1 - \left(\frac{\omega}{\omega_1}\right)^2 + 2i\xi_1 \frac{\omega}{\omega_1}}, \quad H_2(i\omega) = \frac{\omega_2^2}{1 - \left(\frac{\omega}{\omega_2}\right)^2 + 2i\xi_2 \frac{\omega}{\omega_2}}, \tag{7}$$

With ω_1, ξ_1 depending on soil stiffness, their values can be defined according to Seya et al. [20], while ω_2, ξ_2 should be defined to obtain the desired filter behavior at low frequencies.

The signal $B(i\omega)$ is then truncated at the Nyquist frequency to eliminate complex conjugates, and the inverse Fourier transform is applied to obtain $b(t)$, the filtered time-domain signal. This signal is then normalized to achieve a unitary peak ground acceleration (PGA), resulting in the artificial accelerogram $a(t)$, which will be used to compute the artificial pseudo-acceleration spectrum. To match the artificial spectrum S_a^a with a target code-based spectrum S_a, an iterative procedure in the frequency domain is adopted. This frequency-domain spectral matching process is detailed in the following items.

- Define a frequency band $\Delta\vec{\omega}$ and number each band, starting with $k = 1$;
- Initialize the counter $i = 0$;
- Multiply the Fourier transform of a_i (A_i) by the ratio between the mean value of the target spectrum and the mean value of the artificial signal spectrum ($\alpha_{i,k}$) for each frequency band $\Delta\vec{\omega}$:

$$\alpha_{i,k} = \frac{\overline{S_{i,a,k}}}{\overline{S^a_{i,a,k}}} \tag{8}$$

$$A_{i+1,k} = \alpha_{i,k} A_{i,k} \tag{9}$$

  where the overline ($\bar{\cdot}$) denotes the average of the variable, and the subscript k indicates the frequency band;
- Use the inverse Fourier transform on A_{i+1} to obtain the new time-domain signal a_{i+1};
- Determine the pseudo-acceleration spectrum of a_{i+1}, denoted by $S^a_{i+1,a}$, and verify its compatibility with the target spectrum S_a.

The procedure should be repeated until convergence between the target and synthesized spectra is achieved. Figure 1 details the frequency band partitioning scheme employed in this iterative optimization process.

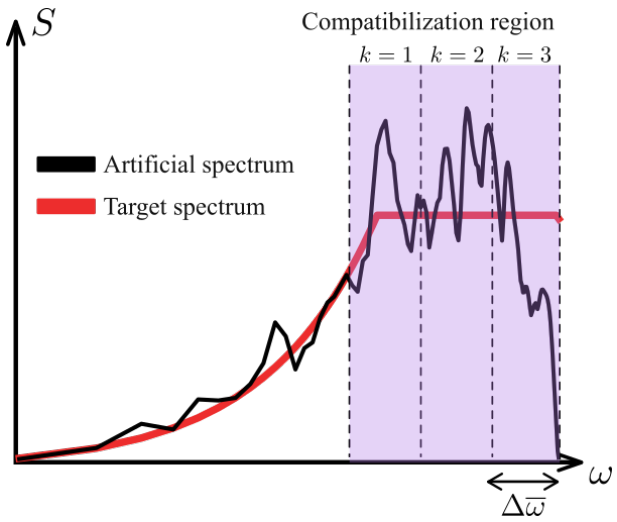


Figure 1. Spectral compatibility between artificial signals and normative design spectra

In this work, the methodology proposed by the authors is modified to minimize the computational time required by the frequency band analysis. For this purpose, it is assumed that the frequency bands are sufficiently narrow such that the average values of the spectra correspond to the analyzed points themselves. Therefore, the expressions can be rewritten as:

$$\alpha_i = \frac{S_{i,a}}{S^a_{i,a}} \tag{10}$$

$$A_{i+1} = \alpha A_i \tag{11}$$

Thus, the value of α can be calculated for all points simultaneously, ensuring a better approximation of the artificial pseudo-spectrum.

3 Generation of Artificial Ground Motion Signal via Proposed Algorithm

This section describes the generation of artificial ground motion records using the proposed algorithm, considering the target spectrum defined by the Brazilian seismic code [21] and real seismic pseudospectra.

3.1 Generation of the Artificial Ground Motion based on NBR 15421:2021 Pseudospectra

To generate an artificial ground motion signal based on the Brazilian seismic code NBR 15421:2021 (Associação Brasileira de Normas Técnicas [21]), it is necessary to define the target response spectrum using the peak ground acceleration (PGA) and terrain class. For this illustrative example, the parameters are defined as follows: $a_g = 0.15g$ and class A. The signal duration is set to 20 seconds, and the number of iterations is set to 20. The resulting artificial accelerogram, along with a comparison between the normative spectrum and the generated spectrum, is presented in Figure 2.

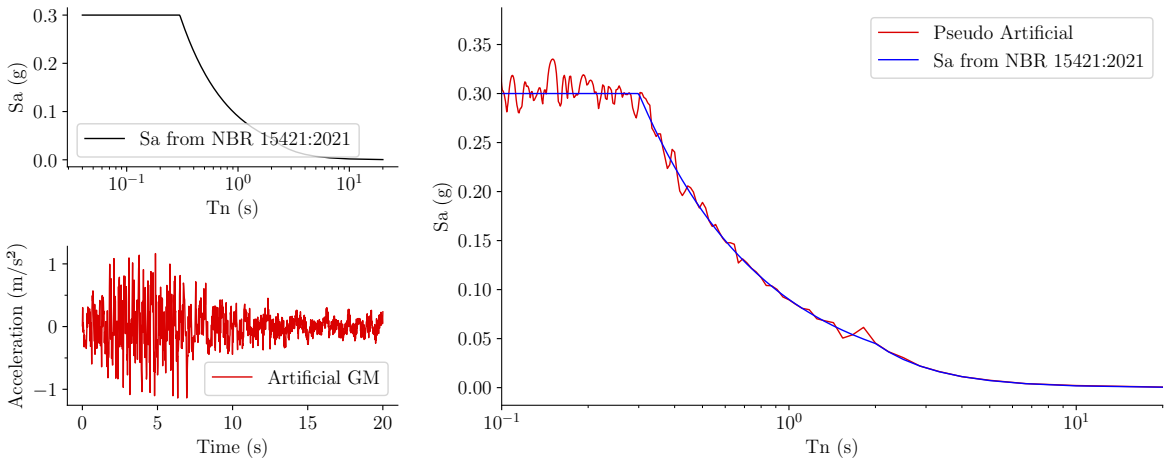


Figure 2. Accelerogram generated from NBR 15421 Pseudospectra

It can be observed that, after applying the methodology presented in this work, the pseudo-acceleration spectrum of the artificial signal closely matches the normative spectrum, which was used as the target in this analysis. Therefore, it can be stated that the proposed methodology enables the generation of artificial ground motion records based on normative spectra.

3.2 Generation Using Real Ground Motion Spectra

In order to evaluate the effectiveness of the proposed methodology in reproducing the target pseudo-acceleration spectrum based on real seismic events, a dataset comprising 12 ground motion records is utilized. This dataset includes a balanced selection of 6 far-field and 6 near-field earthquakes. The characteristics of these recordings are derived from FEMA P695 [22] and are presented in detail in Tables 1 and 2. All corresponding acceleration time histories were retrieved from the PEER-NGA database, ensuring consistency with standardized seismic input data.

Table 1. Summary of earthquake ground motion records: Far-field set [22]

Name	Year	Magnitude	Comp.1	PGAmax (g)	Duration (s)
Chi-Chi, Taiwan	1999	7.6	CHICHI_CHY101-E	0.33	90.00
Duzce, Turkey	1999	7.1	DUZCE_BOL000	0.74	55.90
Kobe, Japan	1995	6.9	KOBE_SHI000	0.22	40.96
Loma Prieta	1989	6.9	LOMAP_CAP000	0.46	40.00
Northridge	1994	6.7	NORTHR_MUL009	0.44	299.90
San Fernando	1971	6.6	SFERN_PEL090	0.22	79.45

Table 2. Summary of earthquake ground motion records: Near-field set[22]

Name	Year	Magnitude	Comp.1	PGAmax (g)	Duration (s)
Denali, Alaska	2002	7.9	ENALI_PS10-047	0.30	92.10
Erzican, Turkey	1992	6.7	ERZINCAN_ERZ-EW	0.38	20.78
Gazli, USSR	1976	6.8	GAZLI_GAZ000	0.60	13.52
Irpinia, Italy	1980	6.9	ITALY_A-STU000	0.21	39.34
Kocaeli, Turkey	1999	7.5	KOCAELI_IZT090	0.23	30.00
Landers	1992	7.3	LANDERS_LCN260	0.65	48.13

A representative example is presented to illustrate the comparison between the original and the synthetic ground motion. The selected case includes the original accelerogram, the corresponding artificial signal with a fixed duration of 20 seconds, and the pseudo-acceleration response spectra of both signals. The number of iterations is set to 20. Figure 3 presents these results.

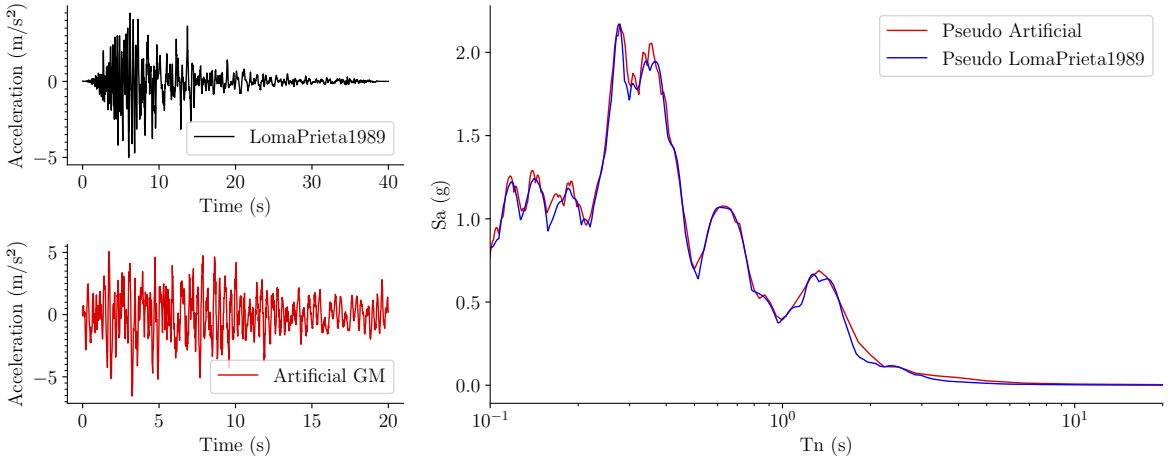


Figure 3. Accelerogram generated from Loma Prieta

It can be observed that, even with a small number of iterations, the peak acceleration and the frequency content of both the real and artificial signals are nearly identical, demonstrating the robustness and computational efficiency of the proposed method. This close agreement suggests that the algorithm successfully captures the essential dynamic characteristics of the original signals without requiring excessive refinement steps. Furthermore, the consistency in frequency content indicates that the method preserves key spectral properties, which is critical for reliable structural response analysis. Tables 3 and 4 summarize the outcomes obtained by applying the proposed methodology to the input signals listed in Tables 1 and 2.

By comparing the real ground motion records with the artificial signals generated using the methodology proposed in this study, it is evident that the predominant frequencies and peak accelerations are very similar. This demonstrates that the methodology is capable of producing artificial signals that preserve the key characteristics of real records, even when the signal durations differ. Regardless of whether the earthquake is far-field (FF) or near-field (NF), the parameters of the artificial signal remain close to those of the real one.The presented results confirm the robustness and flexibility of the proposed methodology when applied to both normative and empirical seismic inputs.

Table 3. Evaluation of Ground Motion Features: Measured Versus Synthesized Signals (FF set).

Signal	f_{pred} real	f_{pred} art	PGA real	PGA art
Chi-Chi,Taiwan	6.14	6.05	0.33	0.35
Duzce, Turkey	3.18	3.10	0.73	0.70
Kobe, Japan	1.51	1.50	0.22	0.20
Loma Prieta	3.63	3.60	0.46	0.52
Northridge	1.90	1.85	0.44	0.44
San Fernando	5.14	5.10	0.22	0.25

Table 4. Evaluation of Ground Motion Features: Measured Versus Synthesized Signals (NF set).

Signal	f_{pred} real	f_{pred} art	PGA real	PGA art
Cape Mendocino	1.50	1.45	0.58	0.45
Erzican, Turkey	3.39	3.45	0.38	0.48
Gazli, USSR	13.80	13.75	0.60	0.66
Irpinia, Italy	2.69	2.75	0.21	0.25
Kocaeli, Turkey	3.41	3.50	0.23	0.25
Landers & 1992	9.42	9.30	0.65	0.65

4 Conclusions

This paper aims to present a methodology inspired by Clough and Penzien [3] for the generation of artificial signals from pseudo-acceleration spectra, whether normative or derived from a real seismic record. Based on the results obtained, it can be concluded that:

- The proposed methodology proves to be effective for the generation of artificial seismic signals from normative spectra;
- It is possible to reproduce the characteristics of a real seismic signal using the proposed methodology;
- The possibility of generating an artificial earthquake that retains the characteristics of the real event, but with reduced duration, is an advantage for performing nonlinear seismic analyses, as it minimizes computational cost;
- The computational cost of using the proposed methodology is minimal, since good approximations can be achieved with a small number of iterations.

Finally, the proposed methodology offers a practical and efficient approach, with low computational cost, for the generation of seismic accelerograms, especially in the context of nonlinear structural analysis.

Acknowledgements. The authors acknowledge the financial support of Conselho Nacional de Desenvolvimento Científico e Tecnológico (CNPq) and Coordenação de Aperfeiçoamento de Pessoal de Nível Superior (CAPES), Brazil.

Authorship statement. The authors hereby confirm that they are the sole liable persons responsible for the authorship of this work, and that all material that has been herein included as part of the present paper is either the property (and authorship) of the authors, or has the permission of the owners to be included here.

References

[1] K. Kanai. An empirical formula for the spectrum of strong earthquake motion. In *Proceedings of the Second World Conference on Earthquake Engineering*, 1961.
[2] H. Tajimi. A statistical method of determining the maximum response of a building during earthquake. PROCEEDING OF WORLD CONFERENCE ON EARTHQUAKE ENGINEERING, 1960.
[3] R. Clough and J. Penzien. *Dynamics of Structures*. Civil engineering series. McGraw-Hill, 1995.
[4] H. Krawinkler and G. Seneviratna. Pros and cons of a pushover analysis of seismic performance evaluation. *Engineering Structures*, vol. 20, n. 4-6, pp. 452–464, 1998.
[5] A. K. Chopra. *Dynamics of structures*. Pearson, 2022.
[6] S. P. Schneider, C. W. Roeder, and J. E. Carpenter. Seismic behavior of moment-resisting steel frames: Experimental study. *Journal of Structural Engineering*, vol. 119, n. 6, pp. 1885–1902, 1993.
[7] P.-H. Wang, K.-C. Chang, D.-C. Dzeng, T.-K. Lin, H.-H. Hung, and W.-C. Cheng. Seismic evaluation of reinforced concrete bridges using capacity-based inelastic displacement spectra. *Earthquake Engineering & Structural Dynamics*, vol. 50, n. 7, pp. 1845–1863, 2021.
[8] X. Long, Z. Chen, and P. Li. Seismic performance of corroded ecc-gfrp spiral-confined reinforced-concrete column. *Polymers*, vol. 16, n. 15, pp. 2110, 2024.
[9] A. Zhang, Z. Chen, J. Liu, X. Ma, and T. Chen. Seismic performance of an innovative cold-formed thin-walled steel–timber composite beam-column joint. *Journal of Constructional Steel Research*, vol. 234, pp. 109742, 2025.
[10] I. U. A. Chy, M. A. G. Fardin, M. R. Awall, and others. Dynamic analysis of cooling tower considering two different column modeling approaches. *Journal of Building Pathology and Rehabilitation*, vol. 10, n. 2, pp. 1–12, 2025.
[11] L. F. F. Miguel, de Oliveira Batista da P. Costa, S. P. Ontiveros-Perez, and Peter de O. A. Souza. Reliability-based simultaneous optimization of quantities, positions, and parameters of inerter-based vibration absorbers to minimize the probability of building failure during earthquakes via the cioa. *Mechanics Based Design of Structures and Machines*, vol. 53, n. 6, pp. 4270–4293, 2025.
[12] G. W. Housner. Characteristics of strong-motion earthquakes. *Bulletin of the Seismological Society of America*, vol. 37, n. 1, pp. 19–31, 1947.
[13] G. N. Bycroft. White noise representation of earthquakes. *Journal of the Engineering Mechanics Division*, vol. 86, n. 2, pp. 1–16, 1960.
[14] M. Shinozuka and C.-M. Jan. Digital simulation of random processes and its applications. *Journal of sound and vibration*, vol. 25, n. 1, pp. 111–128, 1972.
[15] J. Conte and B. Peng. Fully nonstationary analytical earthquake ground-motion model. *Journal of Engineering Mechanics*, vol. 123, n. 1, pp. 15–24, 1997.
[16] Y. Yamamoto and J. W. Baker. Stochastic model for earthquake ground motion using wavelet packets. *Bulletin of the Seismological Society of America*, vol. 103, n. 6, pp. 3044–3056, 2013.
[17] D. D. Chiesa and L. F. Fadel Miguel. Methodology for simulation of the three components of seismic acceleration. *Bulletin of the Seismological Society of America*, vol. 109, n. 6, pp. 2427–2436, 2019.
[18] P. C. Jennings, G. W. Housner, and N. C. Tsai. *Simulated earthquake motions*. California Institute of Technology Pasadena, CA, 1968.
[19] P. Ruiz and J. Penzien. Pseqn: Artificial generation of earthquake accelerograms. *Earthquake Engineering Research Center, Report No EERC*, pp. 69–3, 1969.
[20] H. Seya, M. E. Talbott, and H. H. Hwang. Probabilistic seismic analysis of a steel frame structure. *Probabilistic Engineering Mechanics*, vol. 8, n. 2, pp. 127–136, 1993.
[21] Associação Brasileira de Normas Técnicas. NBR 15421: Projeto de estruturas resistentes a sismos – Procedimento. Standard 15421, ABNT, Rio de Janeiro, Brazil, 2021.
[22] C. A. ATC. Quantification of building seismic performance factors. *Fema*, pp. P695, 2009.